Applied Clay Science 90 (2014) 6–10

Contents lists available at ScienceDirect

Applied Clay Science

journal homepage: www.elsevier.com/locate/clay

Research paper

Electron crystallographic study of a kaolinite single crystal

Ildikó Cora [a,b,*], István Dódony [a], Péter Pekker [b]

[a] Department of Mineralogy, Eötvös Loránd University, 1117 Pázmány P. stny. 1/c, Budapest, Hungary
[b] Institute of Physical Metallurgy, Metalforming and Nanotechnology, University of Miskolc, 3515 Egyetemváros, Miskolc, Hungary

ARTICLE INFO

Article history:
Received 14 March 2013
Received in revised form 30 August 2013
Accepted 27 December 2013
Available online 30 January 2014

Keywords:
Electron crystallography
Structure determination
Kaolinite

ABSTRACT

Kaolinite is an abundant micro- and submicrometer-sized sheet silicate [$Al_2Si_2O_5(OH)_4$] built up of alternating tetrahedral (*T*) and octahedral (*O*) sheets. Except for Neder et al.'s (1999) single-crystal synchrotron study, X-ray and neutron diffraction methods were used for structural measurements on powdered samples. The aim of the present work is to provide a second single crystal structure determination on a kaolinite using recently developed electron diffraction techniques of electron crystallography.

Using precession electron diffraction (PED, Vincent and Midgley, 1994; Avilov et al., 2007) and electron-diffraction tomography (Kolb et al., 2007, 2008) techniques, a 3D diffraction data set was acquired. The crystal structure was determined in SIR2011 and refined in SHELXL97 software. The crystal structure of the studied kaolinite is described in the non-conventional *C*1 space group with unit cell parameters: $a = 5.21(1)$ Å, $b = 9.12(2)$ Å, $c = 7.48(2)$ Å, $\alpha = 88.7(2)°$, $\beta = 104.2(2)°$, $\gamma = 90.3(2)°$.

1. Introduction

Besides the importance of kaolinite in geology and pedology (e.g. Murray, 2000), it also has widespread technical applications in ceramics, paper manufacturing, organoclay nanocomposites or as sorbent for pollutants.

The kaolinite structure was first described by Hendricks (1929) and Pauling (1930). Except for Neder et al.'s (1999) work, there has not been any single crystal based structure determination and refinement on kaolinite carried out so far. Kaolinite is a micro- and submicrometer-sized, "*TO*"-type dioctahedral sheet silicate [$Al_2Si_2O_5(OH)_4$]. Its building units are the "infinite" 2D sheets of corner-sharing SiO_4 tetrahedra forming 6-membered rings and edge-connected $Al_2O_2(OH)_4$ octahedra. These sheets are interconnected by the apical oxygen of the tetrahedral sheets. The three so-called outer hydroxyls of each Al-centered octahedron are at the outer side of the *TO* structural layer and the fourth hydroxyl of an octahedron is located in the middle of the apical oxygen of the hexagonal ring.

Besides theoretical deductions made in the 1930s and 1940s (Brindley and Robinson, 1946; Gruner, 1932) the first experimental structure solution was done by Zvyagin (1960) using oblique texture patterns. Adams (1983) determined the H positions using neutron profile Rietveld refinement technique. All of these studies concluded to a *C*-centered "pseudo-monoclinic" cell. At the same time Suitch and Young (1983) determined and refined all atomic positions of kaolinite in *P*1 sg. (with the same unit cell as in *C*1 sg.) using the Rietveld method applied on powder X-ray and neutron diffraction data sets. They concluded that while the non-H framework has *C*1 symmetry, hydrogen of the inner hydroxyl ions violates the *C*-centering. Electron diffraction studies of kaolinite (Thompson and Withers, 1987; Thompson et al., 1989) confirmed the *C*-centering of the non-H atoms and doubted that the *P*1 sg. Young and Hewat (1988) in their neutron powder diffraction based Rietveld refinement persisted in the *P*1 cell, since inner hydroxyl ions significantly violate the *C*-centering.

Re-refinement of the kaolinite structure was done by several authors using X-ray (Bish and Von Dreele, 1989) and neutron powder techniques (Bish, 1993, at 1.5 K; Akiba et al., 1997, on synthetic deuterated kaolinite sample) and the only single-crystal (synchrotron) data (Neder et al., 1999). All of these studies refer to the *C*1 symmetry of the kaolinite.

All of the experimental works on kaolinite agreed with the *C*1 symmetry of the non-hydrogen framework. Since no reflections violating the *C*-centering ($h + k = 2n + 1$) were documented in the publications referred to above including Suitch and Young (1983) and Young and Hewat (1988), therefore, *P*1 sg. is still questionable.

Simultaneously with the experimental works, *ab initio* quantum chemical calculations on kaolinite structure were published (Benco et al., 2001; Hobbs et al., 1997; Sato et al., 2004). All of these studies focused on the orientation of the OH group in the kaolinite structure and all of the calculations were performed in the *C*1 cell. White et al. (2009) gave a good review of both the experimental and theoretical works on the kaolinite structure that have been conducted so far.

The aim of the present work is to provide the second single crystal structure determination on the typically beam-sensitive kaolinite using the recently developed electron diffraction techniques. These methods proved to be very useful and effective in structure determination of

---

* Corresponding author at: Institute of Physical Metallurgy, Metalforming and Nanotechnology, University of Miskolc, 3515 Egyetemváros, Miskolc, Hungary. Tel.: +36 46 565 111/1749; fax.: +36 46 565 214.
E-mail address: coraildiko@gmail.com (I. Cora).

0169-1317/$ – see front matter © 2014 Elsevier B.V. All rights reserved.
http://dx.doi.org/10.1016/j.clay.2013.12.034

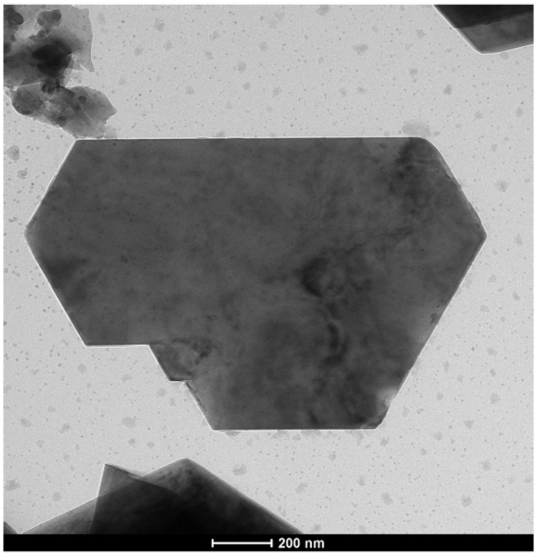

Fig. 1. A kaolinite crystal from Mád on lacey carbon supporting film.

submicron-sized single crystals, such as clay minerals, that could not be studied by conventional single crystal methods.

2. Experimental section

Kaolinite crystals (Fig. 1) of Mád (NE Hungary) kaolin were deposited onto a lacey carbon supporting film from a dilute ethanol suspension. Data collection was carried out in a FEI Tecnai G^2 (X-Twin) transmission electron microscope equipped with a CeB$_6$ filament, operating at 200 kV. A tilt series of selected area electron diffraction (SAED) patterns were recorded on an Eagle CCD camera (2048 × 2048 px, 16 bit). To reduce the strong effect of dynamical scattering on diffracted intensities, we applied the PED technique (precession electron diffraction; recently developed by Vincent and Midgley, 1994; Avilov et al., 2007) using DigiStar (NanoMegas) unit attached to the TEM. The applied precession angle was 1° with 100 Hz precession frequency. To reconstruct the reciprocal space of the measured crystal we recorded tilt series of SAED patterns in precession mode. The acquisition time for each PED/SAED pattern was 2 s. With TEM tomography sample holder it is possible to tilt the crystal in a wide, maximum ±70° tilting range. This method does not require prior orientation of the crystal. The selected crystal in a random orientation is tilted around the tilt axis of the sample holder. The tilt step and the range in our measurement were 1° and ±45°, respectively. The acquired PED patterns were merged into 3D and the *hkl*-intensity data were extracted using the ADT3D diffraction tomography software (Kolb et al., 2007, 2008). A total of 428 reflections were collected ($\geq 4\sigma$) up to a resolution of 0.8 Å, of which 234 are crystallographically independent. The detailed clear description of the applied techniques is available in the paper of Gemmi et al. (2013) and references therein.

The unique advantage of PED compared to the conventional SAED data acquisition is that PED provides quasi-kinematical intensities, i.e. the dynamical scattering is reduced significantly, so the measured intensity is almost proportional to the square of the structure factor (e.g. Own, 2005). The diffraction tomography is an effective technique for 3D diffraction data collection from submicron-sized single crystals. Table 1 summarizes some of the solved and refined structures applying PED and diffraction tomography techniques. The users must pay attention to the possible radiation damage that we minimized by keeping the dose of exposition as low as possible. The measured intensity differences were negligible on the repeated PED/SAED patterns at the same orientation. Since diffracted intensities are proportional to the excited volume, we normalized the measured intensities for the observed flat shaped crystal in the function of tilt values. Based on the observed flat morphology of kaolinite single crystal we supposed that the illuminated volume is approximately cylindrical at zero tilt angle. With tilting the crystal the illuminated volume grows according to the tilting angle. The intensities on the diffraction patterns were corrected accordingly.

In powder methods peak-overlapping, inhomogeneity of the sample (stacking faults, coexistences of polymorphs and polytypes) and orientation of the crystals are crucial disadvantages in contrast to single crystal methods like PED combined with diffraction tomography.

At the end of diffraction data acquisition the measured EDX spectra proved (within 5% rel. error) the unchanged ideal kaolinite composition.

Table 1
Some of the solved and refined structures applying PED and diffraction tomography techniques so far.

Reference	Name	Space group	Number of unique reflections	Resolution [Å]	*R* [%]	Used software for structure determination
Mugnaioli and Kolb (2013)	Natrolite	*Fdd2*	743	0.75	20.2	SIR2008/2011
Mugnaioli and Kolb (2013)	Charoite	*P21/m*	2376	1.15	33.3	SIR2008/2011
Mugnaioli and Kolb (2013)	Charoite	*Pnma*	2666	1.15	19.9	SIR2008/2011
Mugnaioli and Kolb (2013)	ZSM-5	NA	2288	1	38.7	SIR2008/2011
Mugnaioli and Kolb (2013)	IM-5	*Cmcm*	2579	1.2	36.7	SIR2008/2011
Mugnaioli and Kolb (2013)	HKUST-1	*Fm-3m*	2482	1.15	38.8	SIR2008/2011
Mugnaioli and Kolb (2013)	MUF-4l	*Fm-3m*	411	1.3	32.5	SIR2008/2011
Mugnaioli and Kolb (2013)	ECS-3	*Cc*	4417	0.75	28.3	SIR2008/2011
Mugnaioli and Kolb (2013)	ITQ-43	*Cmmm*	2735	1.15	33.8	SIR2008/2011
Gemmi and Nicolopoulos (2007)	Åkemanite	*P-421m*	NA	1	30	SIR2007
Gemmi and Nicolopoulos (2007)	Uvarovit	*Ia-3d*	NA	1.1	12	SIR2007
Gemmi et al. (2011)	Pyroxene	*C2/c*	255	1	31	SIR2008
Hadermann et al. (2010)	$Pb_{13}Mn_9O_{25}$	*P4/m*	NA	0.7	33	SIR2008
Mugnaioli et al. (2009)	Barite	*Pnma*	234	0.8	24-39	SHELX97
Weirich et al. (2006)	$Cs_{0.44}Nb_{2.54}W_{2.46}O_{14}$	*Pbam*	456	1	39.2	SHELX97
Boulahya et al. (2007)	$LaBaCuCoO_{5.2}$	*P4/mmm*	150	1	31.5	SIR2002
Boulahya et al. (2007)	$Ba_6Mn_5O_{16}$	*Cmca*	NA	1	Refinement was not converged	SIR97, SIR2008, SHELX97
Gemmi et al. (2013)	Hemimorphite	*Imm2*	336	0.9	25.5	SIR2008
Gemmi et al. (2013)	Mayenite	*I-43d*	110	0.9	27.4	SIR2008
Gemmi et al. (2013)	$Y_{0.8}Pr_{0.2}Ba_2Cu_3O_7$	*Pmmm*	245	0.9	35.4	SIR2008

NA: not available.